

# Quantum Optics View of Neutron Interferometry

Helmut Rauch

*Atominstytut der Österreichischen Universitäten, A-1020 Wien, Austria*

(Received 6 March 1996; accepted 12 May 1996)

Light and matter wave interference experiments can be analyzed in terms of quantum optics. Correlation and coherence functions provide a proper basis for the description of various coherence phenomena. Squeezed neutron states have been identified in the course of novel postselection experiments which indicates that interference phenomena have to be treated in phase space rather than in ordinary space only. A description in terms of Wigner functions visualize such non-classical quantum states and show the fragility of such Schrödinger-cat-like states against any kind of dissipation, which sheds light on the quantum measurement problem. New projects like neutron Fourier-spectroscopy are intended to broaden the interferometric methods towards condensed matter physics applications.

KEYWORDS: quantum optics, neutron interferometry

## §.1. Introduction

Quantum optics has been developed primarily for light optics where impressive progress in physical experimentation and novel applications has been achieved.<sup>1-3)</sup> Over the last decade it has been shown that quantum optics formalism can be transferred to particle optics where characteristic quantum optical phenomena can open a new horizon for scientific work.<sup>4-7)</sup> The identification of Schrödinger-cat-like states of massive particles and related squeezing phenomena encourages on one hand new epistemological discussions of quantum mechanics and on the other hand opens new possibilities for fundamental and applied research.

Neutron interferometry has become a mature technique for the realization of many quantum optical experiments for massive particles because a neutron carries well defined particle properties and exhibits the wave-particle dualism in any interference experiment.<sup>8,9)</sup> Perfect crystal interferometry uses a Mach-Zehnder geometry with a beam separation of several centimeters. The perfect arrangement of the atoms in a silicon single crystal is used to achieve coherent beam splitting, diffraction, and superposition. (Fig. 1) From simple symmetry considerations it can be understood that the wavefunction for the beam in forward direction (0) behind the interferometer is equally composed of wavefunctions arising from beam paths I and II, which causes a complete modulation of the interference pattern as a function of a phase shift applied to the split beams. Nuclear, electromagnetic, and gravitational interactions, as well as topological effects can cause such a phase shift. Novel results of such measurements will be shown in separate contributions to this conference.<sup>10-12)</sup>

Over the last years, interferometry based upon diffraction from artificially made gratings and layers has been developed which broadens the scope of neutron interferometry and becomes a sensitive testing method for microstructured materials.<sup>13-15)</sup> Additionally, it should be mentioned that Larmor interferometry is another well developed interferometric method which is used in the form of spin-echo instruments in many neutron laboratories.<sup>16-19)</sup> The expert in the field will notice that the quantum mechanical description of a coherent neutron beam by means of coherence functions is rather similar to

the description of the static and dynamical behaviour of atoms in condensed matter by using the van Hove correlation functions.<sup>20,21)</sup>

## §.2. Coherence Properties

In close analogy to the light optical formalism we define the coherence properties of the beam.<sup>1,3)</sup> The first order, two-point-two-time autocorrelation function relating the physical situation at  $(\mathbf{r}, t)$  and  $(\mathbf{r}', t')$  is defined as:

$$G^{(1)}(\mathbf{r}, t; \mathbf{r}', t') = \text{Tr}\{\rho \psi^*(\mathbf{r}, t) \cdot \psi(\mathbf{r}', t')\}, \quad (2.1)$$

where  $\rho$  denotes the density matrix which describes the spatial profile of the beam and its time-dependence in the case of a pulsed beam.  $\psi$  is the solution of the time-dependent Schrödinger equation

$$H\psi(\mathbf{r}, t) = i\hbar \frac{\partial \psi(\mathbf{r}, t)}{\partial t} \quad (2.2)$$

which has the general form

$$\psi(\mathbf{r}, t) \propto \int a(\mathbf{k}, \omega_k) e^{i(kr - \omega_k t)} d\mathbf{k} d\omega_k \quad (2.3)$$

In free space,  $\mathbf{k}$  and  $\omega_k$  are related by the dispersion relation  $\omega_k = \hbar k^2 / 2m$ . Spatial boundary conditions do change  $\mathbf{k}$ , but not  $\omega_k$ , which temporal ones change (diffraction in time<sup>22)</sup>).

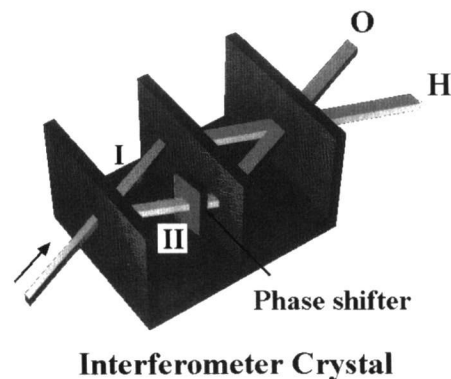


Fig.1. Sketch of a perfect crystal neutron interferometer.

Here we focus on time-independent (stationary) effects, which simplifies the treatment considerably. As in the distinction between elastic and inelastic scattering in condensed matter physics,<sup>20,21)</sup> the stationary situation is obtained by putting  $t - t' = 0$ .  $\omega_k$  now becomes an "Eigenvalue" of the Schrödinger equation and the density of  $k$ -states can be defined as  $g(k) = \int |a(k)|^2 dk$ . The intensity behind the interferometer is given by  $\rho$ , and by the wavefunctions in that region  $R$ , which are composed from wavefunctions arising of both beam paths

$$\psi_0(\mathbf{R}) = \psi_0^I(\mathbf{r}) + \psi_0^{II}(\mathbf{r}'), \quad (2.4)$$

where  $\mathbf{r}$  and  $\mathbf{r}'$  are the optical path lengths to reach the point  $R$  along paths  $I$  and  $II$ , respectively. This gives

$$I_0 = \text{Tr}\{\rho\psi_0^*(\mathbf{R},t)\psi_0(\mathbf{R},t)\} = G^{(1)}(\mathbf{r},t;\mathbf{r},t) + G^{(1)}(\mathbf{r}',t';\mathbf{r}',t') + 2\text{Re}G^{(1)}(\mathbf{r},t;\mathbf{r}',t') \quad (2.5)$$

$G^{(1)}(\mathbf{r},\mathbf{r})$  and  $G^{(1)}(\mathbf{r}',\mathbf{r}')$  denote the intensities when beam path  $I$  or beam path  $II$  is open only ( $I_1$  and  $I_2$ ).  $G^{(1)}(\mathbf{r},\mathbf{r}')$  will be a complex function in general

$$G^{(1)}(\mathbf{r},t;\mathbf{r}',t') = |G^{(1)}(\mathbf{r},t;\mathbf{r}',t')| e^{i\chi(\mathbf{r},t;\mathbf{r}',t')}, \quad (2.6)$$

which defines in its normalized form

$$\Gamma^{(1)}(\mathbf{r},t;\mathbf{r}',t') \equiv \frac{G^{(1)}(\mathbf{r},t;\mathbf{r}',t')}{[G^{(1)}(\mathbf{r},t;\mathbf{r},t)G^{(1)}(\mathbf{r}',t';\mathbf{r}',t')]^{1/2}}, \quad (2.7)$$

the first-order correlation (coherence) function of the related beams. It can be expressed as the Fourier transform of the normalized momentum distribution function

$$\Gamma^{(1)}(\mathbf{r},\mathbf{r}') = \Gamma^{(1)}(\Delta) = (2\pi)^{-3/2} \int g(\mathbf{k}) e^{i\mathbf{k}\cdot\Delta} d\mathbf{k} \quad (2.8)$$

This gives

$$I_0 = I_1 + I_2 + 2\sqrt{I_1 \cdot I_2} |\Gamma^{(1)}(\Delta)| \cos \chi(\Delta), \quad (2.9)$$

where  $\Delta = \mathbf{r} - \mathbf{r}'$  denotes the difference in the optical path lengths along beam paths  $I$  and  $II$ . The interference fringe visibility becomes

$$V = \frac{I_{Max} - I_{Min}}{I_{Max} + I_{Min}} = \frac{2\sqrt{I_1 \cdot I_2}}{I_1 + I_2} |\Gamma^{(1)}(\Delta)|. \quad (2.10)$$

where  $|\Gamma^{(1)}(\Delta)|$  is, misleadingly, often called "degree of coherence". We will show later on that a beam can be completely coherent even when  $|\Gamma^{(1)}(\Delta)|$  becomes zero. The characteristic widths of that function  $|\Gamma^{(1)}(\Delta)|$  define the coherence lengths

$$(\Delta_c^i)^2 = \frac{\int \Delta_i^2 |\Gamma(\Delta_i)| d\Delta_i}{\int |\Gamma(\Delta_i)| d\Delta_i}, \quad (2.11)$$

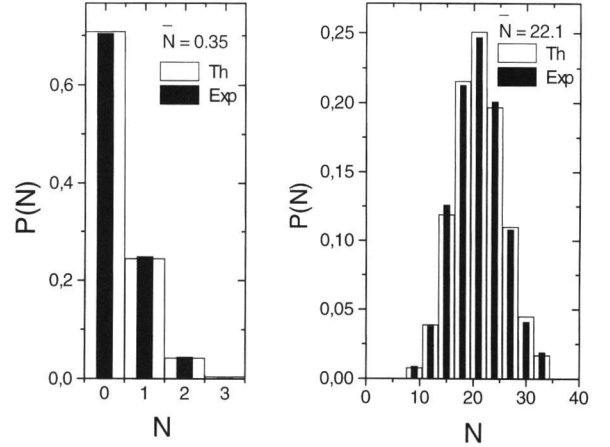


Fig.2. Measured and calculated (dotted) particle distribution function for mean particle number  $\bar{N} \approx 2$  (above) and  $\bar{N} \approx 50$  (below).

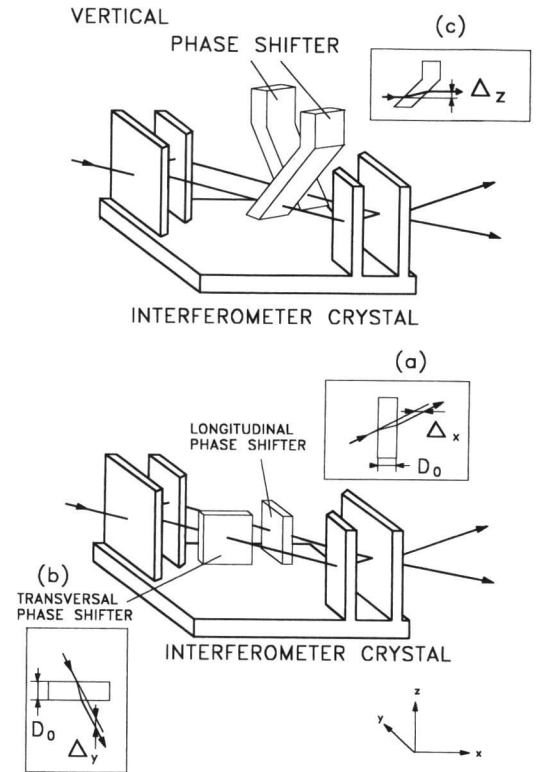


Fig.3. Different phase shifters for phase shifts into different directions.

where  $i = x, y, z$ . In case of Gaussian shaped momentum distributions the coherence functions become Gaussian shaped too, and the momentum widths  $\delta k_i$  and the coherence functions fulfill the minimum uncertainty relation:

$$\Delta_c^i \delta k_i = \frac{1}{2}. \quad (2.12)$$

Such a state in quantum optical terminology is called a coherent state which has the feature of a Poissonian particle distribution

$$P(N) = \frac{\bar{N}^N}{N!} e^{-\bar{N}}, \quad (2.13)$$

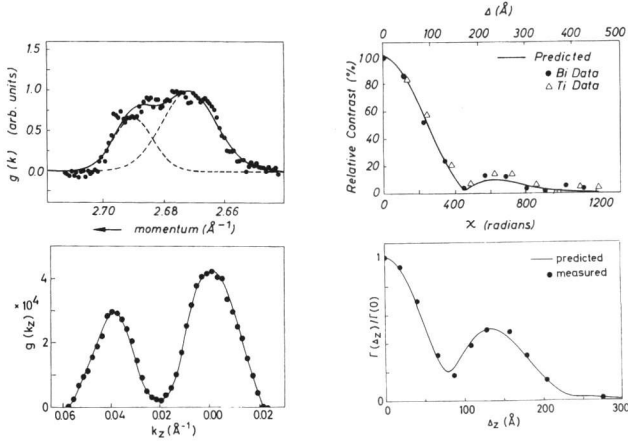


Fig. 4. Measured momentum distribution and measured coherence functions for the longitudinal (above) and vertical (below) direction.

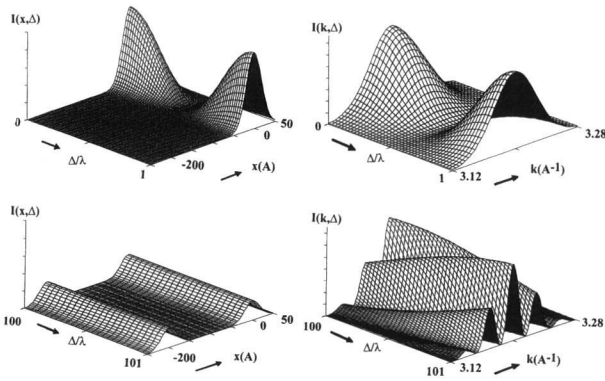


Fig. 5. Wave packet shapes in ordinary and momentum space at low (above) and high (below) interference order.

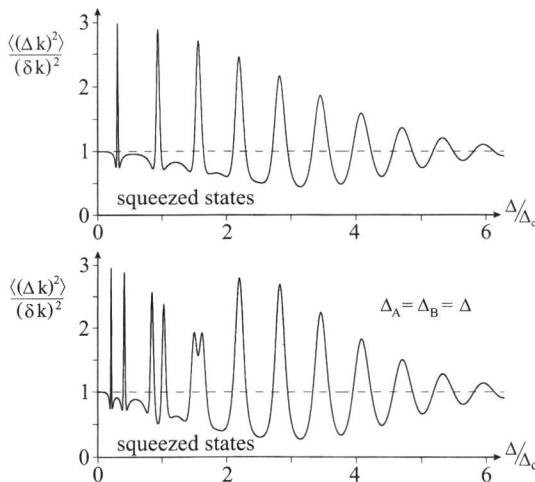


Fig. 6. Squeezing of the momentum distribution for a three- (above) and a four-plate interferometer (below) for  $\Delta k/k_0 = 5\%$ .

as it has been measured recently.<sup>23)</sup> (Fig. 2)

Differently shaped phase shifters (Fig. 3) cause momentum changes into different directions and differences in the optical path lengths. The boundary conditions of quantum mechanics determine the spatial phase shifts for the different cases ( $\chi(\Delta) = k \cdot \Delta$ ):

$$\begin{aligned} \text{Longitudinal:} & \quad D_x = -2\pi N b_c D_0/k \\ \text{Transverse:} & \quad D_y = -2\pi N b_c D_0/k \\ \text{Vertical:} & \quad D_z = -2\pi N b_c D_0 \tan(\varphi)/k \end{aligned}$$

$N$  denotes the particle density,  $b_c$  the coherent scattering length,  $\varphi$  the tilt angle, and  $D_0$  the thickness of the phase shifter. Many measurements of the coherence function have been made in the past which are summarized in a recent paper.<sup>24)</sup> Figure 4 shows the measured momentum distribution in the longitudinal and vertical direction when a twin-monochromator is used in front of the interferometer and it shows the visibility of the interference pattern as a function of the spatial phase shift. The solid lines are the mutual Fourier transforms which verify eq. (2.8). Thus certain coherence properties can be attributed to any beam by its momentum distribution and can be measured directly in an interference experiment. The coherence lengths appear as the widths of the inner (0-order) Fresnel zone of the beam.

### §.3. Schrödinger-Cat-Like States

These are states where an entity occupies at the same time several spatially well separated regions. Such states have been identified in the course of recent neutron interferometric investigations.<sup>7,25)</sup> They appear when the spatial phase shifts become larger than the coherence lengths ( $\Delta \gg \Delta_c$ ). In this case, the interference fringes disappear ( $|\Gamma(\Delta)| \rightarrow 0$ ) and a marked modulation of the momentum distribution appears. In the case of Gaussian distributions the spatial intensity distribution reads as eq.(3.1). and the related momentum distribution becomes

$$I_0(k) \propto \exp[-(k - k_0)^2 / 2\delta k^2] [1 + \cos(k\Delta)], \quad (3.2)$$

which is shown for typical cases in Fig. 5. When one calculates the widths of the related distribution functions  $\langle(\Delta x)^2\rangle = \langle x^2\rangle - \langle x\rangle^2$  and  $\langle(\Delta k)^2\rangle = \langle k^2\rangle - \langle k\rangle^2$ , one notices that  $\langle(\Delta k)^2\rangle$  can become smaller than the coherent state value  $\delta k$  (at  $\Delta = 0$ ), where  $\Delta_c \delta k = 1/2$  is fulfilled. This means in quantum optical terminology interferometric squeezing<sup>26-28)</sup> which even can be strengthened by multiplate interferometers.<sup>29)</sup> (Fig. 6) One emphasizes that a single coherent state ( $\Delta_c \delta k = 1/2$ ) does not exhibit squeezing but a state created by superposition of two

$$\begin{aligned} I_0(x) &= |\psi(x) + \psi(x + \Delta_0)|^2 \\ &= \exp[-x^2 / 2\delta x^2] + \exp[-(x + \Delta_0)^2 / 2\delta x^2] + 2 \exp[-x^2 / 4\delta x^2] \times \exp[-(x + \Delta_0)^2 / 4\delta x^2] \cos(k\Delta), \end{aligned} \quad (3.1)$$

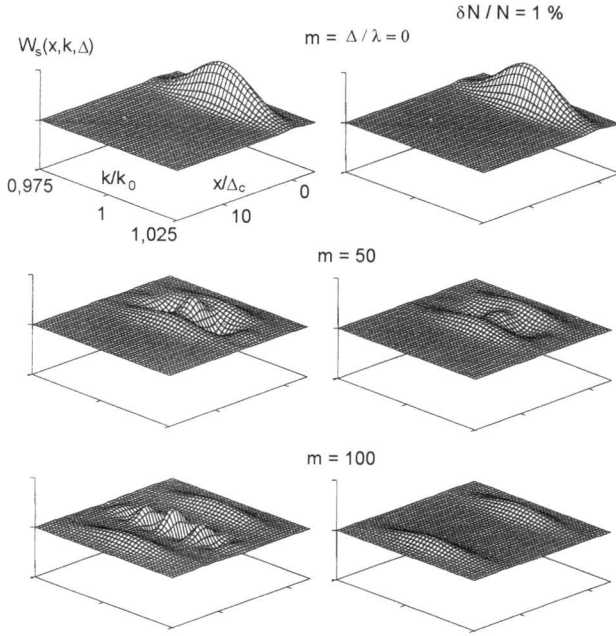


Fig.7. Wigner functions at low (above) and high interference order (below) without (left) and with fluctuations (right).

#### REVERSIBILITY - IRREVERSIBILITY

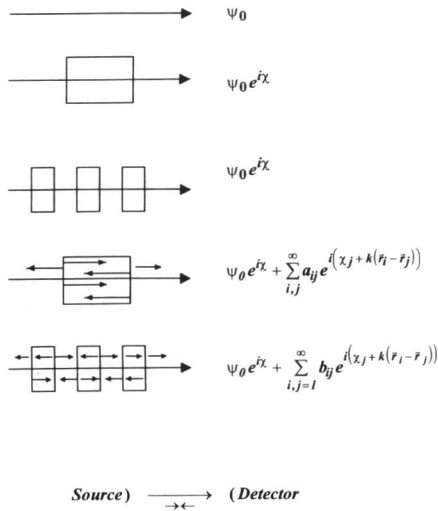


Fig.8. Wavefunction structure from different phase shifters.

coherent states can exhibit a considerable amount of squeezing. These highly non-classical states are made by the power of the quantum mechanical superposition principle.

The existence of such neutron states has been verified recently by a novel momentum state postselection experiment.<sup>25)</sup> First it has been shown that an interference pattern in the region  $\Delta \gg \Delta_c$  can be restored when a narrow

momentum band is filtered out of the beam behind the interferometer by means of an additional analyzer crystal<sup>30)</sup> and it has been shown that a modulation of the momentum distribution appears when this analyzer crystal scans the distribution function.<sup>25)</sup> These highly non-classical Schrödinger-cat-like states are rather fragile against any kind of fluctuations and dissipation effects as we will show in the following chapter.

#### §.4. Wigner representation

In quantum optics many phenomena are visualized by Wigner quasi-distribution functions which are defined as<sup>31,3)</sup>

$$W_s(k, x) = \frac{1}{2\pi} \int_{-\infty}^{+\infty} e^{ikx'} \psi_s^*(x + \frac{x'}{2}) \psi_s(x - \frac{x'}{2}) dx', \quad (4.1)$$

where in our case

$$\psi_s(x) = \psi(x) + \psi(x + \Delta), \quad (4.2)$$

which gives eq.(4.3). Integration over the momentum variable gives the spatial distribution (eq. (3.1)) and integration over the spatial variable gives the momentum distribution (eq.~(3.2)). Typical results are shown in Fig. 7.<sup>32)</sup> When fluctuations of the phase shifter ( $\delta V$  or  $\delta D_0$ ) are included, one notices that the wiggly structure in between the separated peaks is more sensitive at high interference order than at low order. This phenomenon is caused by the statistical fluctuations of the interaction acting on the neutrons inside the phase shifter. It causes a decrease of the coherence and a transition from a quantum state to a mixture. From that consideration upper limits for the separation of massive (Schrödinger-cat) systems due to unavoidable zero-point fluctuations can be given. Thus the extension of quantum "Gedanken" experiments to arbitrarily large distances is unphysical.

#### §.5. Boundary Induced Revival Limits

In various interferometric phase-echo experiments it has been shown that the original contrast can - at least approximately - be revived when a large phase shift ( $\Delta_1 \gg \Delta_c$ ) is compensated by another one ( $\Delta_2 \cong \Delta_1$ ).<sup>33,34)</sup> A more accurate treatment shows that a complete revival of the original wavefunction becomes impossible in principle due to unavoidable splittings of the wavefunction in case of any interaction.<sup>35)</sup> (Fig. 8) This indicates that the complete wavefunction keeps information about all details of interactions the system experienced between the source and the detector. A theoretical treatment has to include the packet structure of the wavefunction and the change of this structure due to the dispersive action of any interaction.

$$W_s(x, k, \Delta) = W(x, k) + W(x + \Delta, k) + 2W(x + \frac{\Delta}{2}, k) \cos(\Delta \cdot k) \\ \propto \exp\left[-\frac{(k - k_0)^2}{2\delta k^2}\right] \times \left\{ \exp\left[-\frac{x^2}{2\delta x^2}\right] + \exp\left[-\frac{(x + \Delta)^2}{2\delta x^2}\right] + 2 \exp\left[-\frac{(x + \Delta/2)^2}{2\delta x^2}\right] \cos(\Delta \cdot k) \right\} \quad (4.3)$$

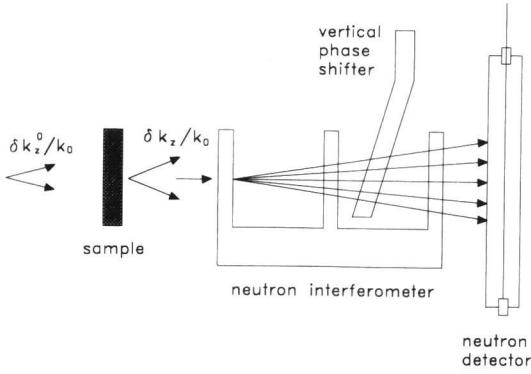
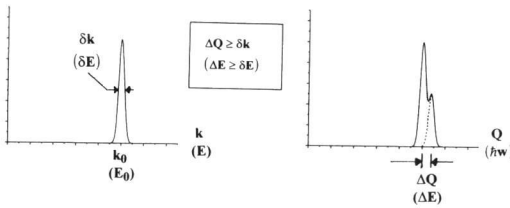


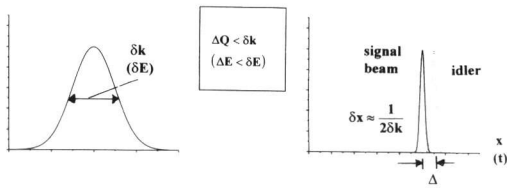
Fig.9. Sketch of an experimental set-up for elastic Fourier neutron spectroscopy.

### SPECTROSCOPY



$$S(\vec{Q}, \omega) \propto \int G(\vec{r}, t) e^{i(\vec{Q}\vec{r} - \omega t)} d\vec{r} dt$$

### FOURIER SPECTROSCOPY



$$|\Gamma(\vec{\Delta}, \Delta t)| \propto \left| \int S(\vec{Q}, \omega) e^{i(\vec{Q}\vec{r} - \omega t)} d\vec{Q} d\omega \right| \propto |G(\vec{r}, t)|$$

Fig. 10. Comparison of standard and Fourier-spectroscopy.

An infinitesimally narrow momentum band only can cross a barrier without losses which generates a more monochromatic transmitted wave which results in a larger coherence length which, step by step, will reach the dimensions of the barriers causing that they act collectively (i.e. enhanced) on the wavefunction. This causes distinct energy bands inside the periodic structure and results in Bragg-like diffractions,<sup>36)</sup> which underlines the statement that a complete revival of the wavefunction behind an interaction region becomes impossible due to typical quantum effects and it shows that irreversibility is a fundamental property of nature.<sup>37-39)</sup>

### §.6. Applications: Fourier Spectroscopy

Coherence properties and phase measurements are the basic features of Fourier spectroscopy and holography. Equation (8) shows that the measurable coherence function is given by the Fourier-transform of the momentum distribution, and from general scattering theory<sup>21,22)</sup> one knows that the angular (momentum) distribution after elastic interaction can be written as a Fourier-transform of the related van Hove correlation function

$$\frac{d\sigma}{d\Omega} \propto S(Q) \propto \int G(\Delta, 0) e^{iQ\Delta} d\Delta. \quad (6.1)$$

Taking into account the momentum distribution of the incident beam  $g(k)$ , which gives  $\Gamma_0(\Delta)$  and the beam attenuation due to parasitic effects, one can measure  $G(\Delta)$  directly<sup>40)</sup>:

$$\frac{|\Gamma(\Delta)|}{|\Gamma_0(\Delta)|} = e^{-\sum_i D} + \left(1 - e^{-\sum_i D}\right) G(\Delta). \quad (6.2)$$

The results in Fig. 4 demonstrate indirectly this feature. Figure 9 shows a sketch of a corresponding set-up. A similar situation exists for time-dependent effects where recently Summhammer *et al.*<sup>41)</sup> have shown how multiple photon exchange between the neutron and an oscillating field can be measured by a temporal Fourier method. In contrast to ordinary Fourier spectroscopy, the momentum (energy) exchange in the target has to be small compared to the momentum (energy) widths of the beam (Fig. 10). Thus a broad incident spectrum is favourable for Fourier spectroscopy, which increases intensity and the spatial and temporal resolution. Related experiments are in progress.

- 1) R.J. Glauber: *Phys. Rev.* 130 (1963) 2529 and 131 (1963) 2766.
- 2) C. Cohen-Tannoudji and S. Haroche: *J. Phys. (Paris)* 30 (1969) 125 and 153.
- 3) D.F. Walls and G.J. Milburn: "*Quantum Optics*", Springer, Berlin 1994.
- 4) E. Muskat, D. Dubbers and O. Schrupf: *Phys. Rev. Lett.* 58 (1987) 2047.
- 5) H. Rauch: *Optik* 93 (1993) 137.
- 6) U. Schmidt, G. Baum and D. Dubbers: *Phys. Rev. Lett.* 70 (1993) 3396.
- 7) H. Rauch: *Phys. Lett.* A173 (1993) 240.
- 8) G. Badurek, H. Rauch and A. Zeilinger (Eds.): "*Matter Wave Interferometry*", *Physica B* 151, Nos. 1-2 (1986), North Holland, Amsterdam 1986.
- 9) V.F. Sears: "*Neutron Optics*", Univ. Press, Oxford 1989.
- 10) G. Badurek: this conference, p. 60.
- 11) Y. Hasegawa, M. Zawisky, H. Rauch and A. Ioffe: this conference, p. 90.
- 12) A.G. Wagh et al.: this conference, p. 73.
- 13) A.I. Ioffe, V.L. Zabayakan and G.M. Drabkin: *Phys. Lett.* 111 (1985) 373.
- 14) M. Gruber, K. Eder, A. Zeilinger, R. Gaehler and W. Mampe: *Phys. Lett.* 140 (1989) 363.
- 15) H. Funahashi, T. Ebisawa, T. Hasegawa, M. Hino, A. Masaike, Y. Otake, T. Tsugachika and S. Tasaki: *Phys. Rev. A* (in print).
- 16) F. Mezei: *Z. Physik* 255 (1972) 146.
- 17) F. Mezei (Ed.): "*Neutron Spin Echo*", Springer Verlag 1980.
- 18) R. Gaehler and R. Golub: *Z. Physik* B65 (1987) 269.
- 19) D. Dubbers, P. El-Muzeini and M. Kessler: *Nucl. Instr. Meth.* A275 (1989) 294.
- 20) L. van Hove: *Phys. Rev.* 95 (1954) 249.
- 21) A.G. Marshall and S.W. Lovesey: "*Theory of Thermal Neutron Scattering*", Clarendon Press, Oxford 1971.
- 22) M. Moshinsky: *Phys. Rev.* 88 (1952) 625.
- 23) M. Zawisky, H. Rauch and Y. Hasegawa: *Phys. Rev.* A50 (1994) 5000.
- 24) H. Rauch, H. Woelwitsch, H. Kaiser, R. Clothier and S.A. Werner: *Phys. Rev.* A53 (1996) 1.
- 25) D.I. Jacobson, S.A. Werner and H. Rauch: *Phys. Rev.* A49 (1994) 3196.
- 26) D.F. Walls: *Nature* 306 (1983) 141.
- 27) W. Schleich, M. Pernigo and Fam Le Kien: *Phys. Rev.* A44 (1991) 2172.
- 28) G.S. Agarwal and D.F.V. James: *J. Mod. Optics* 40 (1993) 1431.
- 29) M. Suda: *Quantum Semiclass. Optics* 7 (1995) 901.
- 30) H. Kaiser, R. Clothier, S.A. Werner, H. Rauch and H. Woelwitsch: *Phys. Rev.* A45 (1992) 31.
- 31) E.P. Wigner: *Phys. Rev.* 40 (1932) 749.
- 32) H. Rauch and M. Suda: *Appl. Phys.* B60 (1995) 181.
- 33) H. Kaiser, S.A. Werner and E.A. George: *Phys. Rev. Lett.* 50 (1983) 560.
- 34) R. Clothier, H. Kaiser, S.A. Werner, H. Rauch and H. Woelwitsch: *Phys. Rev.* A44 (1991) 5357.
- 35) H. Rauch: *Annals of the N.Y. Acad. Sciences* 755 (1995) 263.
- 36) C. Cohen-Tannoudji, B. Diu and F. Laloë: "*Quantum Mechanics*", Vol. I, John Wiley, N.Y. 1977.
- 37) F. Haag: *Comm. Math. Phys.* 123 (1990) 245.
- 38) I. Prigogine: *Proc. Ecol. Phys. Chem.* Elsevier, Amsterdam 1991.
- 39) M. Cini and M. Serva: *Phys. Lett.* A167 (1992) 319.
- 40) H. Rauch: *Physica* B213 & 214 (1995) 830.
- 41) J. Summhammer, K.A. Hamacher, H. Kaiser, H. Weinfurter, D.I. Jacobson and S.A. Werner: *Phys. Rev. Lett.* 75 (1995) 3206.